The distribution of water in degrading polyglycolide. Part I: Sample size and drug release

SUSAN HURRELL, GEORGINA E. MILROY, RUTH E. CAMERON*
University of Cambridge, Department of Materials Science and Metallurgy, Pembroke Street, Cambridge CB2 3QZ, UK
E-mail: rec11@cam.ac.uk

The effect of sample thickness on the degradation of polyglycolide (PGA) disks and on their drug release profiles is explored in this paper, and conclusions drawn about the distribution of water across a sample during degradation. The degradation process was monitored by measuring changes in the long period calculated from small angle X-ray scattering profiles, and by following changes in the pH of the buffer solutions. Drug release profiles were obtained using UV-spectrophotometry. The measurements suggest that reaction-erosion fronts form at the surface of all samples after around 7 days of degradation, and that these fronts progress through the sample at a constant rate of 0.032 mm/day. The data are consistent with a model in which drug is released quickly from the porous, hydrated regions behind the front, and reaches 100% release when the fronts meet.

1. Introduction

PGA is a biocompatible polyester which degrades by hydrolysis to glycolic acid over a period of several weeks. This convenient time scale of degradation makes it a potential candidate as a matrix for controlled drug release. The degradation process becomes more complex as the sample becomes increasingly inhomogeneous; the polymer density, porosity and the concentration of active species vary across the sample, and change with time. This results in a complex interplay between the diffusion rates (of water and reaction products through a changing medium) and the reaction rate (of polymer with water, autocatalyzed by the acidic reaction products). In this paper we investigate how the thickness of disk-shaped samples affects this process, and draw conclusions about the nature of water distribution in PGA at various stages of degradation. In Part II, magnetic resonance imaging techniques are used to image water distribution directly, and test the conclusions drawn.

1.1. The effect of sample size on degradation of polyglycolide-co-lactide

Very few published studies address the issue of the effect of sample size on the degradation of PGA directly. Such literature is discussed in the next section. It is therefore instructive to consider previous studies on the effect of sample size on the related copolymer polyglycolide-co-lactide (PGLA), although the degradation mechanism is likely to differ from that of PGA in its detail [1, 2].

It had been hypothesized that in monolithic samples of PGLA, acidic degradation products can diffuse easily from a thin surface layer. However, significant quantities of acidic degradation products build up in the centre, causing autocatalysis and an increased rate of reaction [3–7]. From this hypothesis, the average molecular weight of thin films and microspheres, which are thinner than the surface layer, would be expected to decrease more slowly than thick samples.

To test this hypothesis, a comparison was made by Grizzi *et al*. [6] between the degradation rates of compression moulded plates of dimensions $15 \times 10 \times 2$ mm, films, microspheres and millimetric beads prepared by solvent-casting, from the same batch of 25% D-lactide, 25% L-lactide, 50% glycolide copolymer. The plates disintegrated more quickly and exhibited a lower average molecular weight in the centre. This effect was not observed for the microspheres, films and beads, and the results therefore support the surface layer hypothesis. However, the millimetric beads degrade more slowly than microparticles and films, which would not be expected from the hypothesis. The results from this experiment may be complicated by the fact that melt-processing and solvent-casting is likely to produce different microstructures, which may also affect the degradation rate.

In a separate experiment, Visscher *et al*. investigated the effect of size on the release of a model drug in microparticles of 25% D-lactide, 25% L-lactide and 50% glycolide copolymer of size ranging between 45 and 177 μm. It was found, as would be expected from the surface layer hypothesis described above, that the larger microparticles degraded more quickly than the smaller ones, although the observed effect was thought to be minimal [8].

These studies on PGLA illustrate how studying the

* Author to whom correspondence should be addressed.

effect of sample size on the rate of degradation can shed light on the mechanisms of degradation, and diffusion of water and degradation products.

1.2. The effect of sample size on the degradation of PGA

The effect of changing the sample size on the rate of degradation in PGA rather than PGLA is rarely addressed in the literature.

Ginde and Gupta found that PGA fibers, formed by melt-spinning, with diameters of 0.155 and 0.203 mm showed no significant difference in degradation rate, while pellets of diameter 3 mm degraded faster than the fibers [9]. However, they attribute this to the anisotropy introduced by melt-spinning causing a decrease in the degradation rate, and not to the size difference.

Tormala *et al*. [10] degraded ''self-reinforced'' PGA rods with diameters ranging from 1.5 to 4.5 mm, which were prepared by sintering bundles of PGA (Dexon) sutures together. The outside surfaces were melted, and the fibers close to the surface fused together. In contrast to the results from pellets and fibers, tensile measurements revealed that the larger rods degraded more slowly which was attributed to the smaller surface to volume ratio, resulting in slower diffusion of water into the samples. It is also possible that the internal structure and porosity of the rods varies with size, and this may also affect the degradation rate.

Results concerning the effects of PGA sample size on degradation rate are therefore inconclusive. This is because, in the experiments reported, additional variables, which may affect degradation rate, are changed in the preparation of samples of different size. However, as illustrated by the studies on PGLA, a consideration of the effect of sample size should give useful information concerning the mechanisms of degradation. These issues are addressed in this paper.

Although PGA has a similar molecular structure to PGLA, and degrades by the same chemical mechanism, its degradation differs from that of PGLA in two important respects [1, 2]. First, PGA is a semicrystalline polymer and the crystalline regions are more resistant to chemical attack. By contrast, PGLA is totally amorphous, thus making hydrolysis of the bulk polymer comparatively easier. Second, instead of thin, porous surface layers and hollow shells, which are observed for PGLA, it is proposed that PGA involves moving reaction-erosion fronts.

It is hypothesized that the degradation process can be separated into four stages [1, 2]. In stage I, small quantities of water diffuse rapidly into the sample (less than 1 wt %). In stage II, little further water is absorbed, but hydrolysis causes the molecular weight to fall. Insertion secondary crystallization, in which new crystals are inserted between existing crystals in the structure, occurs during this stage. This is facilitated by both the presence of water molecules and the decreasing molecular weight, which cause the polymer chains to become more mobile. At the beginning of stage III, a critical molecular weight is reached where oligomers begin to diffuse from the surfaces of the sample. Since the dimensions of the sample are constrained to a certain extent by the semicrystalline structure, the removal of oligomers creates spaces into which water diffuses. A cooperative diffusion of oligomers out of and water into the sample gives rise to fairly sharp reaction-erosion fronts close to the surfaces, in a mechanism analogous to that for the creation of the surface layer proposed for PGLA [3–7]. Behind these fronts, the polymer is hydrated and porous and releases any entrapped drug molecules immediately, whilst ahead of the front, oligomers have yet to diffuse out, the concentration of water is low and drug molecules are trapped in the polymer matrix. During stage III, the fronts move toward the centre of the sample, releasing drug molecules as they go. Stage IV begins when the fronts meet at the centre of the sample, which becomes porous throughout. Fig. 1 illustrates the hypothesized distribution of water in stages I–IV. If this model is correct, the measurements made from disk shaped samples of different thickness should change in predictable ways.

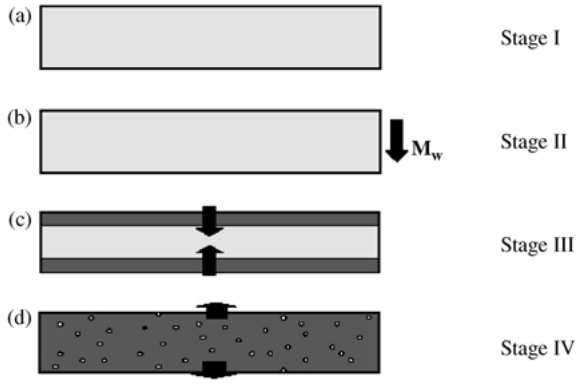

Figure 1 A schematic diagram illustrating the hypothesized water distribution in samples of PGA during stages I–IV.

1.3. Degradation studied by small angle X-ray scattering

In this paper, as previously [1, 2], we use small angle X-ray scattering (SAXS) to monitor the morphological changes of PGA during degradation. The long period is calculated directly from the peak position in the SAXS profiles, and is a measure of the average lamellar repeat in the semicrystalline structure. Two effects contribute to its value during degradation. The long period falls as a consequence of the insertion secondary crystallization that occurs largely in stage II as illustrated in Fig. 3. Conversely, during stage III, the swelling behind the fronts tends to increase the long period. A balance between these effects will be reached at a time close to, but after, the onset of stage III, giving a minimum in the curve of long period with time.

Thick samples reported by King and Cameron [11, 12] show a minimum at 20 days, whilst thin samples reported by Hurrell and Cameron show a minimum at 10 days [1]. Since the long period is an average measurement from the whole sample, this difference is consistent with the proposed mechanism. At a given time, the swollen regions behind the fronts are the same thickness in each sample, but the thicker sample has a greater proportion of unswollen material ahead of the front (Fig. 2) and the average long period will therefore be lower. The

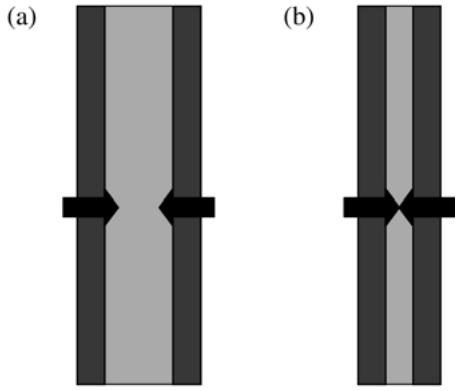

Figure 2 An illustration of the effect of sample thickness on the proportion of material behind the reaction-erosion fronts at a given time of degradation. The reaction-erosion fronts have penetrated the same distance into both disks, but the disk in (a) is thicker than in (b) and consequently, the proportion of the total disk thickness behind the fronts is smaller.

minimum long period, which occurs when the effects of crystallization and swelling balance, will therefore be later.

In this paper a direct study of the effect of sample thickness is made. The data are divided into two parts. First, an investigation is made using the sample preparation techniques used in earlier work to allow direct comparison (Sections 2.1.1 and 2.1.2) with the existing literature. Second, a study is made using samples prepared by a new processing route (Section 2.1.3) in which the sample thickness is better defined and more uniform.

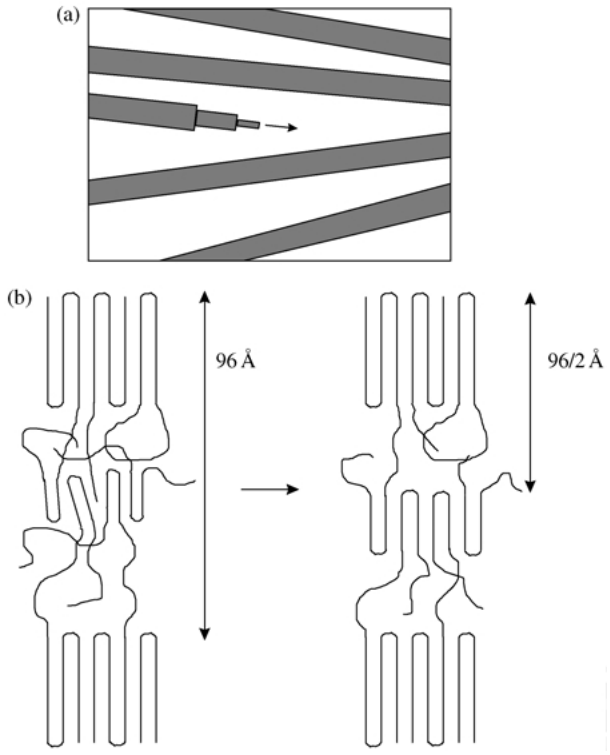

Figure 3 The mechanisms of insertion crystallization. In (a), additional crystalline material grows onto the lateral surfaces of existing crystals between two tilting crystals [13]. In (b), new crystals nucleate from adjacent polymer chains, which are semialigned but not yet crystalline.

2. Experimental

2.1. Sample preparation

PGA was supplied by Alkermes Medisorb Polymer, Ohio, USA, with a quoted inherent viscosity. The inherent viscosity was measured by Alkermes following the guidelines of ASTM D 2857-95, by measuring the relative viscosity of 25 mg PGA in 25 ml hexafluoroisopropanol at $30 \pm 0.1\,^{\circ}C$ in an Ubbelohde type viscometer. The relative viscosity is calculated as the ratio of the average efflux times for polymer solution and pure solvent. The inherent viscosity in dl/g is defined as natural logarithm of the relative viscosity divided by the concentration of the polymer in g/dl.

Method 1

Samples were first made according to the method used by King and Cameron where the PGA pellets had an inherent viscosity of 1.2 dl/g [11, 12]. The pellets were melted at about 230 °C in a copper mould with a PTFE base and then quenched in water. In order to make a drug-loaded sample using this method, the polymer was first ground to a powder and then mixed with powdered theophylline to produce a 4.8 wt % mixture of drug in polymer. The dimensions of the mould were approximately 10 mm × 40 mm, and although the thickness of each sample varied, in the centre it was around 2 mm [11, 12]. The model drug theophylline was obtained from Sigma-Aldrich.

Method 2

Further samples were made according to the method reported by Hurrell and Cameron [1, 2]. The pellets of inherent viscosity 1.2 dl/g were powdered, and samples of either PGA or a 4.8 wt % theophylline-polymer powder mixture of chosen mass were melted in DSC pans on a Linkam hot stage at 236 °C and then quenched into iced water. The samples were removed from the DSC pans. Samples with different masses had the same diameter, and thicknesses were fairly even across the centre of the sample, but tended to be thicker at the edges. Three sizes of sample were prepared. Samples of mass 15 ± 1, 36 ± 1 and 50 ± 1 mg had thicknesses through the centre of the sample of 0.3 ± 0.1, 0.55 ± 0.1 and 0.75 ± 0.1 mm, respectively.

Method 3

A third method of sample preparation was developed which gave samples a uniform and controlled thickness. A different batch of PGA with inherent viscosity 1.3 dl/g was obtained in powdered form. Samples were processed into disks of diameter 15 mm and a chosen thickness using a mould on a hot press. The mould consisted of a top and base made from PTFE-coated aluminum, and an aluminum or steel spacer of chosen thickness with circular holes forming the mould cavity. The base and spacer of the mould were placed on the heated lower plate of a Magnus compressible hot press. The temperature varied across the face of the press, and a thermocouple was used to calibrate the press before and after use. The mould was filled with either PGA powder

or a 4.8 wt % theophylline-polymer powder mixture in stages to ensure that the mould was completely full. Between each stage, the lower and upper plates of the press were brought almost into contact for approximately 1 min to allow the polymer to melt before more polymer was added if required. Once the mould was filled, the second PTFE-coated aluminum foil was placed over the polymer. A pressure of 10 bar at 236 °C was then applied for approximately 30 s. The mould and polymer were then placed immediately into iced water and the samples removed from the mould after cooling. Samples showed a slight rippling on the surface.

Irrespective of the preparation method used, the thicker samples were more difficult to quench to an amorphous microstructure because they cooled more slowly in the iced water. Thicker samples therefore tend to be slightly more crystalline.

All samples were degraded, without agitation, at 37 °C in phosphate buffered saline of pH 7.4 and concentration 0.01 M. The solutions, bottles and equipment were autoclaved at 120 °C and 10^5 Pa pressure for 30 min before use.

For the SAXS experiments, samples made using method 1 were degraded in 50 ml of buffer, whilst samples made using method 2 used a 1.8 mg sample mass: 1 ml buffer volume ratio to determine the quantity of buffer needed for different sample thicknesses. For drug release experiments, a 0.36 mg sample mass: 1 ml buffer volume ratio was used for different sample thicknesses made using methods 1 and 2. For all samples made by method 3, a 6 mg sample mass: 1 ml buffer volume mass ratio was used for different sample thicknesses, and this applied to all samples used in SAXS and drug release experiments.

2.2. Small angle X-ray scattering

Small angle X-ray measurements of the wet degraded samples were taken on station 8.2 at the Daresbury Laboratory synchrotron radiation source. The data were collected on a quadrant detector over intervals of 30 s, and then normalized using an ionization chamber placed after the sample, to correct for fluctuations in the beam intensity and sample thickness. The intensity was also divided by the response of the detector to a uniform illumination from a ^{55}Fe source. Background scattering was subtracted and the *x*-axis was calibrated using wet rat-tail collagen. The Lorentz correction was applied to convert the scattering data to that from a single lamellar stack. The long period was calculated from the peak position of the Lorentz-corrected data using the Bragg equation.

2.3. Drug release and pH

The concentration of theophylline in the buffer solution was measured at intervals during degradation using a UVIKON 860 double beam spectrophotometer. Absorbance measurements were taken at 271 nm and the values were entered into the Beer–Lambert equation to calculate the amount of theophylline release. For the samples made using methods 1 and 2, buffer was returned to the sample bottles after each measurement. However, for samples made using method 3, the buffer was diluted by mass, and not returned to the sample bottles.

The pH of the solutions was measured using indicator strips from Sigma-Aldrich with ranges from 4.5 to 10.0 and 7.0 to 14.0 and an accuracy of 0.5. All sample bottles were shaken before the readings were taken.

3. Results

3.1. Results from samples made by methods 1 and 2

The average long period of samples prepared using method 1 [11, 12] (thickness very approximately 2 mm) appear in Fig. 4 alongside results from samples of weight 36 mg (thickness approximately 0.55 mm) prepared using method 2 [1, 2]. The initial long periods and the minimum values are similar, but the minima occur at about 20 days and 10 days, respectively. The rise in the long period after the minimum is slower in the thicker sample. To explore this effect further, samples were prepared using method 2 with a range of thicknesses. Fig. 5 shows the long periods calculated from samples of masses 15 and 50 mg (thickness approximately 0.3 and 0.75 mm). Once again the long period minimum occurs later in the thicker samples.

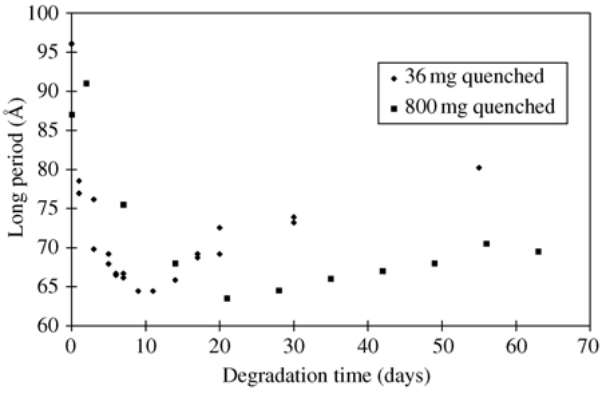

Figure 4 Long period changes with degradation from 800 mg samples, made using method 1, and 36 mg quenched samples, made using method 2. The long period minimum occurs at a later degradation time for the thicker 800 mg samples, and the subsequent rise in long period is slower. The experimental error is ± 1 Å.

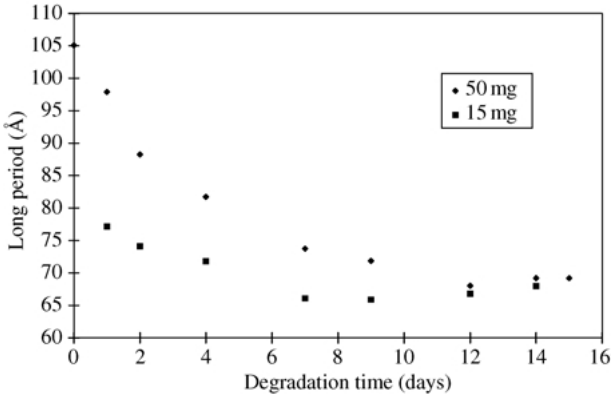

Figure 5 Long period changes with degradation from 15 to 50 mg samples, made using the method 2. The long period minimum occurs at later degradation times for thicker samples. The experimental error is ± 1.4 Å.

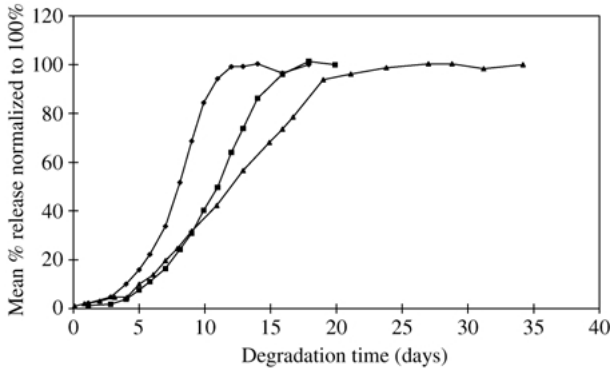

Figure 6 Fractional drug release profiles from 15 mg (diamonds), 50 mg (squares) and 800 mg (triangles). All samples are made using method 1. Slower release is shown from thicker samples. The experimental error is ± 2.5% of the value of each experimental point.

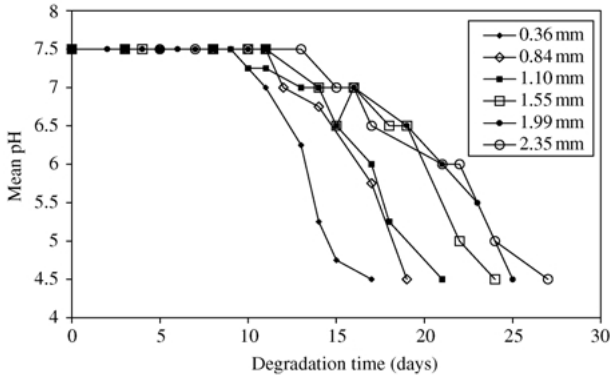

Figure 8 pH variation with degradation for quenched disks, 15 mm diameter and varying thickness, with samples made by method 3. The pH begins to fall at about 13 days for each thickness but the fall is slower for thicker samples. The experimental error is ± 0.35 pH units.

The drug release profiles from samples prepared using methods 1 and 2 are shown in Fig. 6. The thicker samples show a slower drug release.

To obtain more quantitative information on the effect of sample thickness, further experiments were performed on samples prepared using method 3 in which the sample thickness was uniform and well controlled.

3.2. Results from a series of samples prepared using method 3

Fig. 7 shows the SAXS long period of a series of samples prepared using method 3. The curves have been offset for clarity. As before, the average long period minimum occurs later in thicker samples, and the subsequent increase in the long period is slower.

Fig. 8 shows the pH of the buffer solutions as a function of sample immersion time. After a certain time, the buffer capacity is reached and the pH begins to fall. The ratio of the amount of buffer solution to the mass of the sample was held constant for all samples. It is clear from Fig. 8 that the pH starts to fall at much the same time irrespective of sample thickness. However, the pH drops more slowly in the buffer containing thicker samples.

Fig. 9 shows the percentage drug release from a series of samples prepared using method 3. As before, the fractional release is slower in the thicker samples. Because of the controlled thickness of these samples, it is possible to calculate a cumulative absolute drug release per unit surface area of the sample. The resulting curves superimpose until release is complete, which occurs at earlier times for thinner samples (Fig. 10).

The results from the series of samples prepared using method 3 are therefore consistent with those from samples prepared according to methods 1 and 2. However, the controlled and uniform thickness allows for a more quantitative discussion.

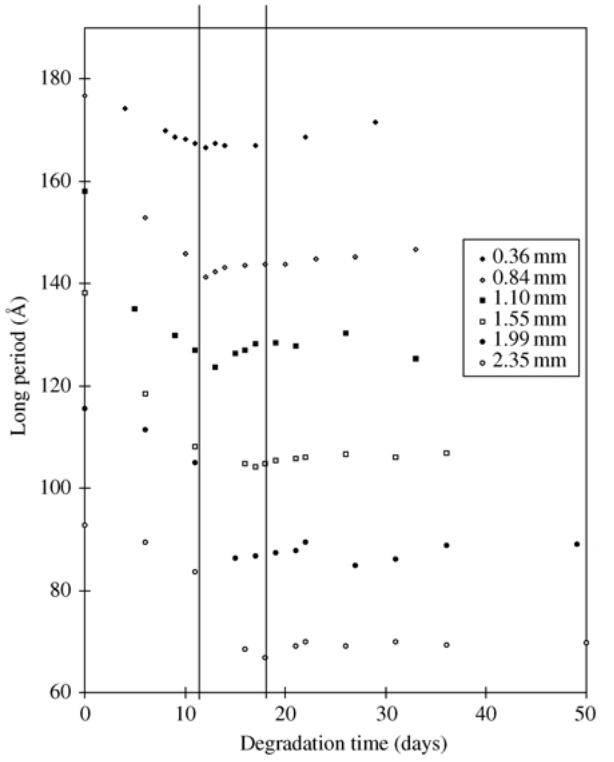

Figure 7 Long period changes with degradation for quenched disks, 15 mm diameter and varying thickness, with samples made by method 3. The long period minimum occurs at later degradation times for thicker samples, and the subsequent increase in the long period is slower. The graphs are offset by 20 Å increments for clarity. The experimental error is ± 1.5 Å.

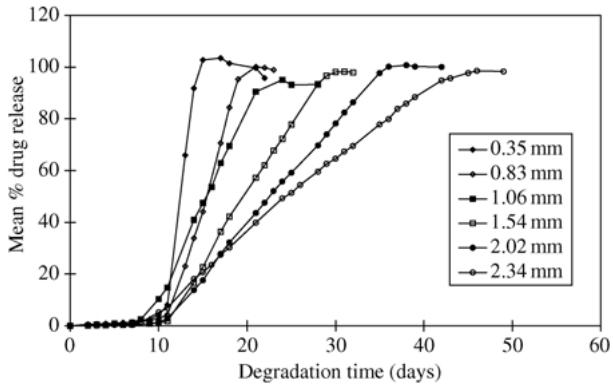

Figure 9 Profiles showing fractional drug release from quenched disks, of 15 mm diameter and varying thickness, with samples made by method 3. Drug release starts at about 9 days for all thicknesses, but the rate of fractional drug release is smaller for thicker samples. The experimental error is ± 8.5% of the value of each experimental point.

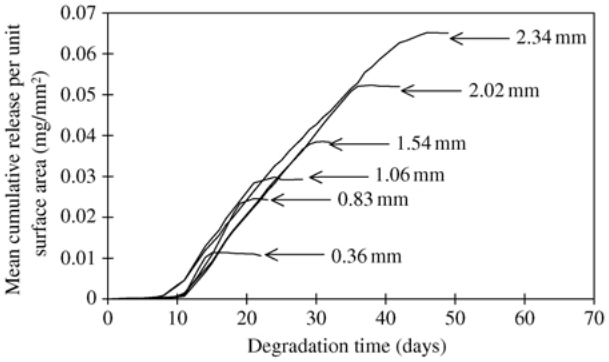

Figure 10 Profiles showing cumulative absolute release per unit surface area for quenched disks, of 15 mm diameter and varying thickness, with samples made by method 3. Drug release starts at about 9 days for all thicknesses, and the rate of release is also the same for all thicknesses, with thicker samples finishing later. The experimental error is $\pm$ 8.5% of the value of each experimental point.

4. Discussion

The samples prepared using methods 1 and 2 give a qualitative indication of the effects of sample thickness. Thicker samples show a later minimum in the long period (Figs. 4 and 5) and drug release occurs at a later time (Fig. 6). However, one should be cautious about drawing detailed conclusions about degradation and release kinetics from the shapes of these curves because of the poor control of geometry achieved using these methods of sample preparation. The samples are not of uniform thickness and this will have an effect on the measurements. A more detailed consideration of the degradation mechanism is now made, using the data from samples made using method 3, which have uniform thicknesses.

Stage I is diffusion-controlled, and will therefore be strongly affected by the thickness of the sample. However since we believe that this diffusion occurs quickly in comparison with the timescale of the degradation, it is anticipated that this will not have a strong effect. Once water has diffused through the bulk of the sample by the beginning of stage II, hydrolysis will occur at the same rate regardless of sample size, until the critical molecular weight is reached.The reaction-erosion fronts, whose appearance marks the onset of stage III, should therefore start at the same time in samples of different size. Two aspects of the results confirm this suggestion. First, the cumulative absolute drug release per unit surface area starts at approximately the same time irrespective of size, in Fig. 10. The start time only varies between 7 and 11 days, and this variation is thought to be an experimental feature of the measurements. Second, the pH of the buffer solution starts to fall at approximately the same time for each sample (Fig. 8). The fall in pH occurs when the buffer capacity is reached, due to large quantities of glycolic acid being released into the buffer solution as the fronts move through the sample. The time at which the pH starts to decrease varies between 10 and 15 days, again due to the inherent scatter of the data. These times occur slightly later than those at which the drug release starts. It is believed that the fall in pH of the buffer solution starts a short time after the onset of stage III, but that drug release is more sensitive to changes in the polymer during stage III and so starts almost immediately. This issue is addressed later in this section. The model also predicts that once the fronts have begun, they progress at the same rate through the sample, irrespective of size. This condition means that at a given time, thicker samples should have a greater proportion of unswollen material ahead of the reaction-erosion fronts. This hypothesis is confirmed by five pieces of data.

First, the minimum in the average long period occurs at later times in the thicker disk samples (Fig. 7). The minimum occurs when the effects of insertion crystallization throughout the sample are balanced by the swelling behind the reaction-erosion front. Therefore, since thicker samples have a greater proportion of unswollen material, it takes longer to reach this minimum. Second, the subsequent rise in average long period is slower in thicker disk samples (Fig. 7). This result again is a consequence of the larger fraction of unswollen material ahead of the front at any given time. Third, when the ratio of buffer volume to sample mass is held constant, the pH falls more slowly in buffer solutions containing thicker samples (Fig. 8). This finding is again a consequence of the smaller proportion of the material releasing acidic degradation products in the thicker samples. Fourth, the profiles in Fig. 9 show the rate of fractional drug release is lower for thicker samples. The four-stage model predicts that drug release starts at the onset of stage III and occurs as the reaction-erosion fronts move inwards from the sample surface and finish when they meet in the centre. Therefore, at a given time after the start of release, the proportion of the total distance moved by the reaction-erosion fronts from the sample surface, and therefore the proportion of the total amount of drug released from the regions behind the fronts, will be less for thicker samples. Fifth, the cumulative absolute release profiles from PGA disks in Fig. 10 show the onset and rate of cumulative absolute release are independent of sample thickness: the release is approximately linear (zero-order) after the initial onset of release (after about 9 days), and the profiles superimpose on each other until full release is reached. This result is expected because release occurs from the regions behind the reaction-erosion fronts as they progress into the sample, and the model predicts that the fronts start and move at a rate independent of sample thickness. The drug release from the disk samples prepared by method 3 (Fig. 9) starts slightly later than from the samples prepared by method 2 (Fig. 6). This discrepancy is probably due to the difference in sample processing.

Finally the model predicts that stage IV, which starts when the reaction-erosion fronts meet in the centre of the sample, should occur at later times for thicker samples. This hypothesis is confirmed by the drug release data. The cumulative drug release profiles in Fig. 10 show that the drug release finishes at later times for thicker samples. This effect occurs because the drug release finishes when the fronts meet in the centre of the sample at the end of stage IV, and consequently, will finish later for thicker samples.

It is worth considering in more detail the variation between sample thicknesses and the time of onset of stage III measured by the SAXS, pH and drug release data in Figs. 7–10. The SAXS long period minimum,

related to the onset of stage III, occurs at later times for thicker samples. In contrast, the pH starts to fall at about 13 ($\pm$ 2) days regardless of sample thickness (although the data is quite scattered). The drug release begins at about 9 ($\pm$ 2) days degradation time, which again is independent of sample thickness. The differences in these observations is believed to be a consequence of differences in the way that the SAXS, pH and drug release techniques measure changes to the polymer at the onset of stage III.

The long period minimum occurs when the effect of insertion crystallization (which causes the long period to decrease) and sample swelling (which causes the long period to increase) balance. Swollen polymer is found behind the reaction-erosion front, so to deliver the amount of swelling needed to balance the effect of insertion crystallization on the average long spacing, the fronts need to penetrate a critical proportion of the sample. As mentioned in Section 1.2, the reaction-erosion fronts should progress at the same rate for all sample thicknesses, so it will take thicker samples longer to achieve this critical penetration than thinner samples, giving a later long period minimum as is observed in Fig. 7. In other words, the long period minimum occurs at a short time after the start of stage III, so it does not directly represent its onset.

The pH and drug release data both suggest that the onset of stage III is independent of sample size. These observations agree with the prediction made by the four-stage degradation model, because unlike SAXS, these two techniques are not affected by the fraction of material ahead of the front. However, whilst drug release predicts that stage III starts after 9 ($\pm$ 2) days, the pH data predicts that stage III starts after 13 ($\pm$ 2) days. This discrepancy is thought to occur because when the polymer changes at the onset of stage III, drug release starts almost immediately afterwards, whereas, it takes slightly longer for enough glycolic acid to diffuse from behind the fronts of the polymer and overcome the buffer capacity and cause its pH to fall.

Therefore, all the data are consistent with a model in which the fronts form some time after initial immersion, and move at a constant rate from the surface to the centre of the sample. The drug is released quickly from the swollen region behind the fronts where the polymer is open and porous. Drug release is thus thought to be complete when the fronts meet at the centre of the sample.

Further analysis allows the onset of stage III be determined more accurately. Drug release finishes for a sample of given thickness when the fronts from each side meet in the centre of the sample. Thus, the distance moved by each front at this time is half the sample thickness. Since we have drug release data from samples of different thickness, a plot of distance moved by each reaction-erosion front against time may be constructed by plotting half the sample thickness against the time of total release (Fig. 11). A straight line was chosen to fit the data but it is acknowledged that a curved line could provide an equally good fit. However, the data in Part II adds strong support to the use of a straight line graph.

From the graph, the x-intercept suggests that the reaction-erosion fronts start at 7 ($\pm$ 3) days, and the

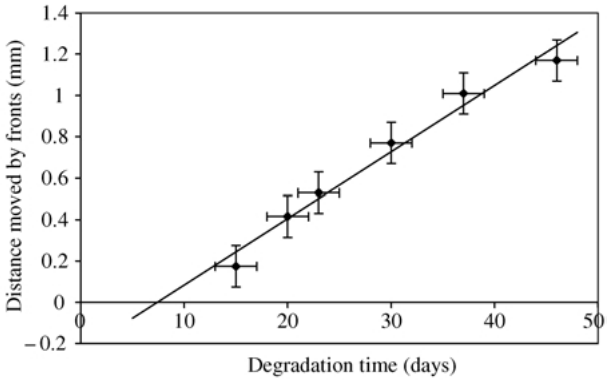

Figure 11 A plot showing the dependence of time of complete drug release on disk thickness. This indicates that reaction-erosion fronts start at about 7 ($\pm$ 3) days and move in from the sample surface at a linear rate of 0.032 ($\pm$ 0.004) mm/day.

gradient indicates that the speed of front movement is 0.032 ($\pm$ 0.004) mm/day. Therefore, it is believed that the true onset of stage III starts at around 7 days, and that the experimental techniques used in this research predict a slightly later onset because of the time taken for the effects to become apparent. This time varies according to the technique used, as demonstrated in this chapter.

The apparent linear movement of the fronts as suggested by Fig. 11 is also noteworthy. The plot of distance moved by the reaction-erosion fronts against degradation time demonstrates that Fickian diffusion is not obeyed. The reaction-erosion front model is similar in some ways to that of Case II diffusion, in which solvent plasticizes the polymer and allows greater swelling behind the sharp fronts, and the kinetics exhibited are linear with time. However, the movement of the reaction-erosion fronts in polyglycolide is not an example of Case II diffusion because the timescales are wrong: previous work has shown that low levels of water penetrate the polymer, causing plasticization, over a timescale much less than 7 days, the time when reaction-erosion fronts start [1]. The kinetics associated with the movement of the reaction-erosion fronts are discussed further in Part II.

5. Conclusions

The use of PGA samples with a regular, controllable geometry has allowed a more thorough investigation into PGA degradation using SAXS, pH and drug release. The data from samples of different thickness were consistent with the four-stage model proposed for the degradation of polyglycolide. It appeared that reaction-erosion fronts began at the same time, and progressed linearly through the sample at the same rate irrespective of sample size. It is only the onset of stage IV, when the reaction-erosion fronts met in the centre of the sample, that showed size dependence, with the onset time increasing for thicker samples. The data were also consistent with a model in which the drug diffused quickly from the more open material behind the fronts and in which 100% release was achieved when the fronts met. For polyglycolide with the molecular weight studied here, the fronts began at about 7 ($\pm$ 3) days and moved at a rate of 0.032 ($\pm$ 0.004) mm/day.

Acknowledgments

The authors are grateful to Pfizer Ltd and the EPSRC for financial support, and to Dr Julie Richardson and Dr Hiep Huatan for help and advice. The X-ray experiments were carried out at Daresbury Laboratory with the assistance of Dr Nick Terrill.

References

1. S. HURRELL and R. E. CAMERON, *J. Mater. Sci. (Mater. In Med.)* **12** (2001) 811.
2. S. HURRELL and R. E. CAMERON, *ibid.* **12** (2001) 817.
3. S. M. LI, H. GARREAU and M. VERT, *ibid.* **1** (1990) 123.
4. S. M. LI, H. GARREAU and M. VERT, *ibid.* **1** (1990) 131.
5. S. M. LI, H. GARREAU and M. VERT, *ibid.* **1** (1990) 198.
6. I. GRIZZI, H. GARREAU, S. LI and M. VERT, *Biomaterials* **16** (1995) 305.
7. M. VERT, S. M. LI, G. SPLENLEHAUER and P. GUERIN, *J. Mater. Sci. (Mater. In Med.)* **3** (1992) 432.
8. G. E. VISSCHER, J. E. PEARSON, J. W. FONG, G. J. ARGENTIERI and R. L. ROBISON, *J. Biomed. Mat. Res.* **22** (1988) 733.
9. R. M. GINDE and R. K. GUPTA, *J. Appl. Polym. Sci*., **33** (1987) 2411.
10. P. TORMALA, H. M. MIKKOLA, J. VASENIUS, S. VAINIONPAA and P. ROKKANEN, *Die Angewandte Makromolekulare Chemie* **185** (1991) 293.
11. E. KING and R. E. CAMERON, *J. Appl. Polym. Sci.* **6** (1997) 1681.
12. E. KING, S. ROBINSON and R. E. CAMERON, *Polym. Int.* **48** (1999) 15.
13. G. STROBL, ''The Physics of Polymers'' (Springer, Berlin, 1996).

Received 1 November 2001
and accepted 20 August 2002